

Chemical preparation of ultra-fine aluminium nitride by electric-arc plasma

G. P. VISSOKOV, L. B. BRAKALOV

Higher Institute of Chemical Technology, Bul. "Kl. Ohridski" No. 8, 1156 Sofia, Bulgaria

Ultra-fine aluminium nitride has been obtained by interaction of aluminium and nitrogen in electric-arc plasma. It has been proved that the rate determining step of the process is the evaporation of the aluminium powder. The most appropriate thermodynamic and kinetic conditions for obtaining pure, finely dispersed product has been determined. The prepared aluminium nitride has dimensions of about 50 nm and specific surface of up to $100 \text{ m}^2 \text{ g}^{-1}$. The items made by the baking of this product at 1600 K have zero porosity. The product has a greater chemical reactivity than the one produced by conventional methods.

Nomenclature

a	weight content of nitrogen in the product (%)	T_{pb}	particle melting point (K)
c_p	specific heat of the particle ($\text{J kg}^{-1} \text{ K}^{-1}$)	T_{pv}	particle evaporation temperature (K)
d_p	particle diameter (m)	v_g	rate of the gas (m sec^{-1})
d_{p0}	initial particle diameter (m)	α	degree of nitride formation (%)
G_p	current particle weight (kg)	α_T	heat transfer coefficient between the gas and the particle ($\text{W m}^{-2} \text{ K}^{-1}$)
G_{p0}	initial particle weight (kg)	α_v	evaporation coefficient (1 in this case)
L_{pb}	particle melting heat (J kg^{-1})	β	degree of evaporation (%)
L_{pv}	particle evaporation heat (J kg^{-1})	$\Delta\tau_b$	time for particle melting (sec)
M_g	molecular weight of the gas	ρ_g	density of the gas (kg m^{-3})
M_p	molecular weight of the particle	ρ_p	density of the particle (kg m^{-3})
P_g	gas pressure (Pa)	ρ_{pl}	density of the particle in liquid state (kg m^{-3})
P_v	vapour pressure of the particle (Pa)	σ_{gv}	mean diameter of the molecule in the gas–vapour system (m)
S	specific surface ($\text{m}^2 \text{ g}^{-1}$)	τ_b	the time for which the particle reaches melting point (sec)
s_c	course of the particle (m)	τ_r	relative residence time
s_p	coefficient of friction resistance of the particle	τ_v	time necessary for the full evaporation of the particle (sec)
T_g	gas temperature (K)		
T_p	particle temperature (K)		
T_{g0}	mean temperature of the reactor (K)		

1. Introduction

The physical and chemical properties of aluminium nitride (high boiling point*, good insulating properties at high temperature, hardness, great wear resistance, chemical stability) make it a material of interest for high-temperature technology. The

addition of aluminium nitride to aluminium and sintered-metal alloys quickly enhances their elasticity and refractoriness. Ultra-fine aluminium nitride is of great interest for the production of low-porous articles in powder metallurgy.

Aluminium nitride is prepared nowadays by

*The data concerning boiling point are very contentious (they range from 2500 to 2800 K), and this is easily explained by the fact that AlN decomposes before reaching the boiling point.

direct interaction of aluminium with nitrogen or ammonia. The carbo-thermal reactions of Al_2O_3 in a nitrogen atmosphere, or reduction of Al_2O_3 in a hydrocarbon and nitrogen medium, is used comparatively more rarely [1]. The aluminium nitride prepared in this way has low specific surface (less than $0.5 \text{ m}^2 \text{ g}^{-1}$). The items made from it are sintered at a high temperature (2200 K) and have considerable porosity (more than 5%). Therefore, conventional methods cannot provide for the preparation of aluminium nitride suitable for use in powder metallurgy. The need for a preparation method producing more dispersed and with lower sintering point aluminium nitride brings many researchers to synthesize it from the gas phase by means of a plasma jet [2–13]. This product, however, does not meet the requirements for dispersity, purity and conversion degree. The experimental conditions used in these researches, and the low degree of conversion of the reagents, make the realization of those processes difficult.

In order to find appropriate reagents for a high degree of conversion we carried out a comparative analysis of the known thermodynamic data [1, 12–14] and the data obtained by us when determining the reaction equilibrium:



For determining the equilibrium conversion in Reaction 1 we used the modified Tyomkin–Schwarzmann method [15]. This method takes into account the phase transitions of reagents at equilibrium. The results (Fig. 1, Curves 1 to 4) and their comparison to those of other researchers (Fig. 1, Curves 5 and 6) show that the optimum conversion (100% practically) into AlN, in regions of plasma technology temperatures

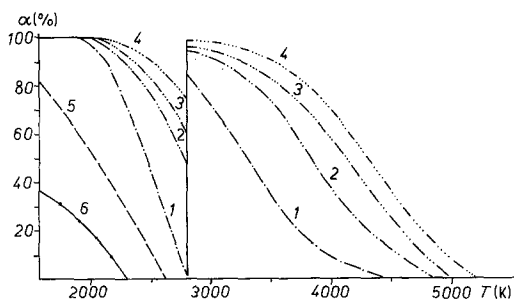


Figure 1 Calculated thermodynamic values of the degree of nitride synthesis (α) as a function of temperature: 1 – $\text{Al/N} = 1:1$; 2 – $\text{Al/N} = 1:10$; 3 – $\text{Al/N} = 1:20$; 4 – $\text{Al/N} = 1:30$; 6 – $\text{Al/N/Cl/H} = 2:30:6:90$ [14]; 5 – $\text{Al/N/Cl/H} = 2:400:6:1200$ [14].

(2500 to 3500 K), is obtained by its direct synthesis from elementary aluminium and nitrogen.

On the basis of the thermodynamic analysis we decided to synthesize pure, highly dispersed aluminium nitride from powder-like aluminium and nitrogen.

Today it is generally accepted that the rate determining step of heterogeneous plasma and chemical processes is the evaporation of the most refractory condensed phase [16–19]. A major effect of this supposition is that one must ensure not only the relevant thermodynamic conditions (temperature and reagents ratio), but also adequate residence time of the particles in the reactor so that they evaporate completely. Such conditions allow the desired product to be prepared in gaseous phase. After appropriate swift cooling of the reaction mixture the product can be prepared in the required highly dispersed form. These considerations necessitate modelling of the particle evaporation process. The following equations recommended in [16–19] are used for calculating the following.

1. The rate of change of the particle diameter in the case of sublimation or particle temperature lower than the evaporation temperature:

$$\frac{dd_p}{d\tau} = -2.368 \times 10^{-19} \frac{(M_p^{-1} + M_g^{-1})^{1/2}}{\rho_p \sigma_{gv}^2} M_p \times P_v (2P_g + P_v) \frac{T_g + T_p}{A d_p} \quad (2)$$

where

$$A = 1.736 \times 10^{-16} \frac{1 + M_p M_g^{-1}}{\alpha_v \sigma_{gv}^2} \frac{T_g + T_p}{d_p} + 1$$

2. The rate of change of the particle diameter with particle temperature equal to the evaporation temperature:

$$\frac{dd_p}{d\tau} = - \frac{2\alpha T}{L_{pv} \rho_{pl}} (T_g - T_{pv}) \quad (3)$$

3. The linear speed of the particle:

$$\frac{ds_c}{d\tau} = v_g [1 - \exp(-\tau/\tau_v)] \quad (4)$$

where

$$\tau_v = \frac{4 d_p \rho_p}{3 s_p v_g \rho_g}$$

4. The rate of change of the particle temperature with the latter lower than its melting point:

$$\frac{dT_p}{d\tau} = \frac{6\alpha_T}{c_p \rho_p d_p} (T_g - T_p) \quad (5)$$

5. The rate of change of the particle temperature with the latter higher than its melting point:

$$\frac{dT_p}{d\tau} = \frac{6\alpha_T}{c_p \rho_{pl} d_p} (T_g - T_p) + \frac{L_{pv}}{2 c_p d_p} \frac{dd_p}{d\tau} \quad (6)$$

6. The time for particle melting:

$$\int_{\tau_b}^{\tau_b + \Delta\tau_b} \alpha_T (T_g - T_{pb}) d\tau = 0.167 d_{p0} \rho_p L_{pb} \quad (7)$$

The system of Equations 2 to 7 has been solved with the aid of the program RKF45 [20]. The Runge–Kutta–Fehlberg method has been used in this program for solving the system of ordinary differential equations [21]. In the solution we assumed that the reactor is isothermal – an approach which does not lead to an essential error in this case [19]. When modelling the process the most unfavourable case of evaporation – that in which the particles used in the experiment have largest diameter (50 μm) – has been taken into account.

It is necessary that the particle residence time in the reactor (τ_p) is related to the time necessary for its full evaporation (τ_v), for one and the same temperature in the reactor when determining the impact of the evaporation kinetics on the degree of conversion. That is why the quantity of relative residence time (τ_r) has been used:

$$\tau_r = \tau_p / \tau_v \quad (8)$$

For determining τ_p the system of Equations 2 to 7 has been solved with the following initial conditions: $d_p = 50 \mu\text{m}$; $s_c = 0 \text{ m}$; $T_g = T_{g0}$; $\tau = 0 \text{ sec}$; $T_p = 300 \text{ K}$. The time necessary for particle full evaporation has been determined from the solution of the system when $d_p = 2.1 \times 10^{-10} \text{ m}$ – the diameter of the aluminium nitride molecule.

Besides the relative residence time the degree of evaporation (β) has also been introduced:

$$\beta = (G_{p0} - G_p) \times 100 / G_{p0} (\%) \quad (9)$$

The degree of nitride synthesis (degree of change of the basic aluminium into AlN), and the specific surface of the aluminium nitride, as the most important, basic characteristics of the prepared product, have been determined. The nitrogen content of the product has been determined using

the method of Keldal [1], and the degree of nitride synthesis (α) by the formula:

$$\alpha = 100a/34.15 (\%) \quad (10)$$

The specific surface has been determined by the Klyatchko–Gourvitch method [22], based on the low-temperature adsorption of air at 77.4 K. The temperature of the plasma jet and the reactor has been determined on the basis of energy balance.

2. Experimental procedure

The experiments were carried out using the equipment described previously [23]. Aluminium powder (99.99% purity) was injected at a rate of $7 \times 10^{-3} \text{ g sec}^{-1}$ into the end of the active part of the arc from the vibratory-feeder by means of nitrogen (99.99% purity). The size of the particles was between 25 and 50 μm and the specific surface was $3.5 \text{ m}^2 \text{ g}^{-1}$. Argon or a mixture of nitrogen and argon was used as the plasma-forming gas. The experiments were carried out in two stages: in a cold-wall (CW) reactor and in a hot-wall (HW) reactor. The CW reactor is a copper heat exchanger (0.04 m in length) cooled with water. The temperature of its inside wall is about 650 K. This causes high radial and axial temperature gradients. The HW reactor is made of refractory ceramics and is housed in a water-cooled case. The temperature of its inner wall is about 2000 K. It has a more homogeneous temperature field than the CW reactor.

Three series of experiments in the CW reactor were carried out with a flow rate of plasma-forming argon of $7.08 \times 10^{-4} \text{ m}^3 \text{ sec}^{-1}$ and an aluminium to nitrogen of 1:30, 1:35 and 1:40 (mol: mol). Three series of experiments in the HW reactor were carried out also with an aluminium to nitrogen of 1:30 and different flow rates of plasma-forming argon; 4.72×10^{-4} , 7.08×10^{-4} and $9.44 \times 10^{-4} \text{ m}^3 \text{ sec}^{-1}$.

Further, the impact of the cooling rate on the reaction mixture in the cooling equipment was studied. A heat exchanger providing a cooling rate of $dT/d\tau \sim 2 \times 10^5 \text{ K sec}^{-1}$ was used after the CW reactor, and after the HW reactor a cooling rate of $dT/d\tau \sim 8 \times 10^5 \text{ K sec}^{-1}$ was used.

3. Results and discussion

The results obtained for the degree of conversion (Fig. 2) show that with an increase of temperature to about 3300 to 3800 K, and of the dimensionless residence time to about 0.98 to 1.03 (log

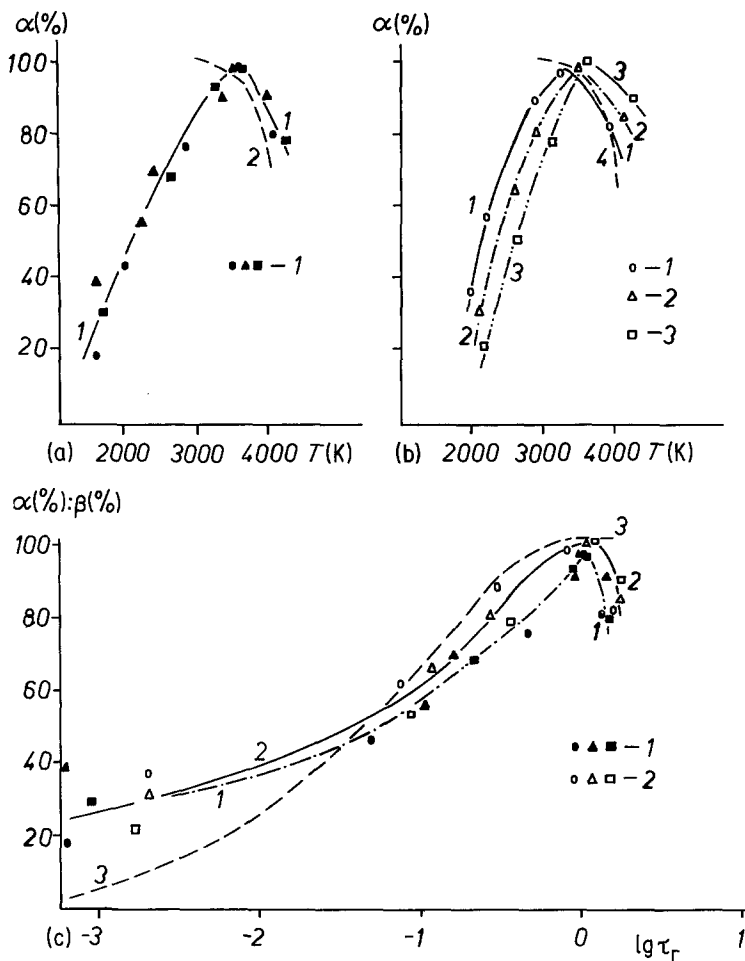


Figure 2 Dependence of the degree of nitride synthesis (α) on the temperature of the (a) cold-, and (b) hot-wall reactor, and the dependence of the degree of nitride synthesis (α) and the degree of evaporation (β) on the logarithm of the dimensionless residence time of the aluminium particles ($\lg \tau_r$) with $d_{\text{mean}} = 50 \mu\text{m}$ (c). (a) 1 – for CW reactor with consumption of plasma-forming gas, argon, of $7.08 \times 10^{-4} \text{ m}^3 \text{ sec}^{-1}$ and Al:N equal to 1:30 (●), 1:35 (▲) and 1:40 (■). 2 – equilibrium degree of nitride synthesis at Al:N = 1:30. (b) 1 – HW reactor with consumption of plasma-forming gas, argon, of $4.72 \times 10^{-4} \text{ m}^3 \text{ sec}^{-1}$ (○); 2 – $7.08 \times 10^{-4} \text{ m}^3 \text{ sec}^{-1}$ (△); 3 – $9.44 \times 10^{-4} \text{ m}^3 \text{ sec}^{-1}$ (□) and permanent mol ratio Al:N = 1:30; 4 – equilibrium degree of nitride synthesis. (c) Dependence of the degree of nitride synthesis for: 1 – CW reactor (●, ▲, ■); 2 – HW reactor (○, △, □). 3 – dependence of the degree of evaporation. For all experiments the consumption of powder-transporting gas, nitrogen, was $1.11 \times 10^{-4} \text{ m}^3 \text{ sec}^{-1}$.

$\tau_r = -0.05$ to 0.07), the conversion increases to the maximum (about 100%) after which it decreases. The comparison of the degree of nitride synthesis (α) (Fig. 2c, Curves 1 and 2) and the degree of evaporation (β) (Fig. 2c, Curve 3) shows that for relative residence times less than or equal to one they are similar and almost coincide quantitatively. For residence times greater than that necessary for particle evaporation ($\tau_r > 1$) the experimental degree of nitride synthesis determined almost coincides with the thermodynamic one (Fig. 2a, Curves 1 and 2 and Fig. 2b, Curves 1 and 4). These facts show undoubtedly that Reaction 1 is limited by the evaporation rate of the condensed phase. The difference in the degree of nitride synthesis, on the one hand, and the theoretical thermodynamic degree of conversion and the theoretical degree of evaporation on the other, besides the assumed approximations in Equations 2 to 7, are probably due to additional factors. For relative residence times $\tau_r \leq 0.08$ (Fig.

2c) the degree of nitride synthesis is greater than the theoretical degree of evaporation, probably because of the measurable rate of Reaction 1 in heterogeneous conditions. For $0.08 \leq \tau_r \leq 1.03$ the lower degree of nitride synthesis is probably due to the condensation of AlN from the gaseous phase on the still evaporating aluminium particles. This increases the particle evaporation temperature and decreases the degree of evaporation of the particles. For $\tau_r \geq 1.03$ the conversion degree is greater than the theoretical value (Figs. 2a and b) probably for the continuing reaction in the cooling equipment in heterogeneous conditions. The difference in the conversion degree in the various reactors (Fig. 2c, Curves 1 and 2) is determined by the more unfavourable temperature condition in the CW reactor. The particles, entering wall areas, evaporate to a considerably lesser degree at this temperature than at the theoretical one corresponding to the reactor temperature. The lower degree of evaporation determines the lower degree

of conversion in the CW reactor. The presence of this "wall" effect is the reason that the conversion degree does not reach 100%.

The results for the dependence of specific surface on temperature and residence time (τ_r) are similar (Fig. 3). They unambiguously show that for the same cooling conditions of the reaction mixture, the size of the specific surface is determined by the degree of particle evaporation (Fig. 2c, Curve 3) for $\tau_r \leq 1.05$ (Fig. 3c). The cooling rate in the cooling equipment determines the largest possible surface of the product for $\tau_r \approx 1$. This, as well as the "wall" effect and the greater temperature gradients in the CW reactor, where the reagent cooling rate is significantly lower, is the cause of the considerably smaller surface as compared to the case of HW reactor (Fig. 3c) for the same relative residence time. The decrease in specific surface with the increase in temperature at $\tau_r \geq 1$ is the result of accelerated coagulation and baking of particles in the cooling equipment

because of its greater temperature, which is again due to the low cooling rate. The specific surface of the product can be significantly increased by increasing the cooling rate. Thus, in additional tests with a cooling rate of $dT/dr \sim 10^7 \text{ K sec}^{-1}$, aluminium nitride with a specific surface of about $200 \text{ m}^2 \text{ g}^{-1}$ and a conversion degree of practically 100% is obtained.

The plasma-chemically synthesized aluminium nitride is a highly dispersed powder which is light grey in colour. The results from chemical, X-ray and spectral analyses show that the nitride is similar in structure to the stoichiometric material and its basic impurities are excess aluminium and oxygen. The results from electron micrograph analysis show that the particles have spherical form and presumably uniform particle size. The basic fraction has a diameter of 40 to $50 \mu\text{m}$. Due to its high dispersion this nitride is distinguished physically and chemically from that obtained by conventional methods. The fine

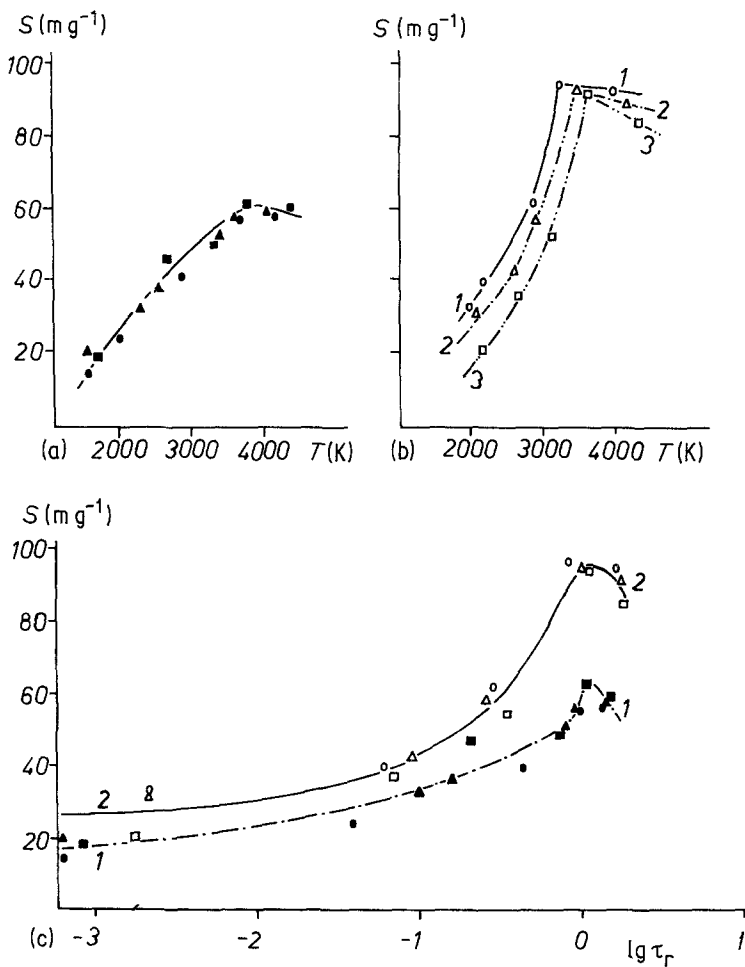


Figure 3 Dependence of the product specific surface (S) on the temperature of the (a) cold-, and (b) hot-wall reactor, and on the logarithm of the dimensionless residence time of the aluminium particles (τ_r) with $d_{\text{mean}} = 50 \mu\text{m}$ (c). (a) For CW reactor with consumption of plasma-forming gas, argon, of $7.08 \times 10^{-4} \text{ m}^3 \text{ sec}^{-1}$ and a Al:N ratio of 1:30 (●), 1:35 (▲) and 1:40 (■). (b) for HW reactor with permanent mol ratio Al:N = 1:30 and consumption of plasma-forming gas, argon, of: 1 - $4.72 \times 10^{-4} \text{ m}^3 \text{ sec}^{-1}$ (○); 2 - $7.08 \times 10^{-4} \text{ m}^3 \text{ sec}^{-1}$ (△); 3 - $9.44 \times 10^{-4} \text{ m}^3 \text{ sec}^{-1}$ (□). (c) 1 - CW reactor (●, ▲, ■); and 2 - HW reactor (○, △, □). For all experiments the consumption of powder-transporting gas, nitrogen, was $1.11 \times 10^{-4} \text{ m}^3 \text{ sec}^{-1}$.

dispersion determines the chemical reactivity of the powder obtained and this exhibits itself in the interaction with humid air. It has been established that with continuous exposure to atmospheres with 100% relative humidity aluminium nitride is completely hydrolysed to hydroxide and ammonia. It has been found that baking of ultra-dispersed samples of aluminium nitride begins at 1000 K and at 1600 K the samples reach zero porosity. The reduction of the optimal baking temperature of the plasma-synthesized aluminium nitride is determined by its extraordinary high activity due to the large specific surface (60 to $100\text{ m}^2\text{ g}^{-1}$) and the structure defects fixed during the swift cooling. These properties allow the utilization of aluminium nitride prepared in this way in the production of items with very good exploitation features by the methods of powder metallurgy.

4. Conclusions

With the present research the direct synthesis of ultra-dispersed aluminium nitride in electric-arc plasma is achieved. With a temperature up to 3500 K the process occurs by evaporation of aluminium and synthesis of aluminium nitride in the gaseous phase and on the phase boundary by diffusion. The rate determining step of the process is the evaporation of the aluminium powder. A product with practically 100% purity, with diameter of its spherical particles less than 60 nm, and specific surface up to $100\text{ m}^2\text{ g}^{-1}$, can be obtained using the plasma-chemical technique. Baked at a maximum temperature of 1600 K the samples have zero porosity. The cooling equipment used does not provide a sufficient cooling rate. For the synthesis of a more dispersed product, cooling by injecting cold gaseous jets (argon or nitrogen), may be recommended. One can conclude from the data presented that the product with maximum dispersity and purity could be obtained at temperatures of 2900 to 3400 K and relative residence times of $\tau_r = 1.0$ to 1.1.

References

1. G. V. SAMSONOV, O. P. KOULIK and S. V. POLISHCHUK, "Polutchenie i Metody Analiza Nitridov" (Naoukova dumka, Kiev, 1978) p. 360.
2. A. N. KRASNOV and V. M. SLEPTZOV, *Poroshkovaya Metallurgiya* 5 (1965) 79.
3. O. MATSUMOTO, Y. SHIRATO and T. MIYAZAKI,

- J. Electrochem. Soc. Jpn.* 36 (1968) 207.
4. O. MATSUMOTO, Y. SHIRATO and Y. HAYAKAVA, *ibid.* 37 (1969) 151.
5. G. L. LONG and J. FOSTER, *J. Amer. Ceram. Soc.* 42 (1959) 53.
6. S. VEPREK, C. BRENDL and H. SCHATER, *Z. Naturforsch.* 24a (1969) 2025.
7. V. M. ZAKE, V. E. LIEPINYA, V. K. MELNIKOV, T. N. MILLER and U. A. ZIELEN, *Izv. AN Latv. SSR, Serya Fiz. Techn. Naouk* 22 (1970) 73.
8. A. A. ASHEOULOV, M. G. BERDITCHEVSKIY, F. M. KUZMENKOVA, V. A. SIDOROV, S. A. BOURENKOV, G. V. KURTOUKOV, A. A. KORNILOV and V. V. MAROUSIN, "Nizkotemperaturnaya Plasma v Technologii Neorganicheskikh Veshchestv" (Naouka, Novosibirsk, 1971) p. 25.
9. Japanese patent No. 75 499/73 (1973).
10. T. SATO and M. ITAWA, *Nippon Kagaku Kaishi* 15 (1973) 1869.
11. A. M. SVIDOUNOVITCH, V. V. PETCHKOVSKIY, F. M. KUZMENKOVA, V. A. SIDOROV and S. A. BOURENKOV, *Voprosy Himii i Himicheskoi Technologii* 40 (1975) 148.
12. D. P. ZETKEVITCH and N. V. ZAHOJIJ, "Materialy i Izdeliya Poloutchaemuye Metodam Poroshkovej Metallurgii" (Naoukova dumka, Kiev, 1975) p. 78.
13. D. P. ZETKEVITCH, Y. P. GRABIS, G. N. MAKARENKO, T. Y. KOSOLAPOVA and T. N. MILLER, *Poroshkovaya Metallurgiya* 17 (1977) 1.
14. Yu. N. MAMONTOV, A. L. SOURIS and S. N. SHORIN, Sb. "II Vsesoyuznyy Simpozium Po Plasmohimii", t. Vol. 2, tezisyu dokladov, (Zinatne, Riga, 1975) p. 186.
15. L. P. ROUZINOV and B. S. GOULENITZKI, "Ravnovesnyye Prevrashcheniya v Metallurgicheskikh Reaktsiyah", (Naouka, Moscow, 1975).
16. D. M. TCHIZHIKOV, Yu. M. TZVETKOV and I. K. TAGIROV, Sb. "Termodinamika i Kinetika v Protzessov Vosstanovleniya Metallov" (Naouka, Moscow, 1972) p. 7.
17. S. A. PANFILOV, I. K. TAGIROV and Yu. V. TZVETKOV, Sb. "Generatoruy Nizkotemperaturnoy Plazmuy" (Energiya, Moscow, 1969) p. 48.
18. D. M. TCHIZHIKOV, Yu. V. TZVETKOV and I. K. TAGIROV, Sb. "Mehanizm i Kinetika Vosstanovleniya Metallov" (Naouka, Moscow, 1970) p. 49.
19. Yu. V. TZVETKOV and S. A. PANFILOV, "Nizkotemperaturnaya Plazma v Protzessah Vosstanovleniya" (Naouka, Moscow, 1980) p. 146.
20. L. F. SHAMPINE, H. A. WATTS and S. M. DAVENPORT, *SIAM Rev.* 18 (1976) 376.
21. E. FEHLBERG, *Computing* 6 (1970) 61.
22. A. KLYATCHKO-GOURVITCH, *Izv. AN SSSR OHN* 35 (1961) 1884.
23. G. P. VISSOKOV, K. D. MANOLOVA and L. B. BRAKALOV, *J. Mater. Sci.* 16 (1981) 1716.

Received 21 June
and accepted 29 November 1982